Nuclear Instruments and Methods in Physics Research A 765 (2014) 91–98

Contents lists available at ScienceDirect

Nuclear Instruments and Methods in Physics Research A

journal homepage: www.elsevier.com/locate/nima

# Double-sided super-module R&D for the ATLAS tracker at HL-LHC – A summary

A. Clark [e,*], G. Barbier [e], F. Cadoux [e], M. Endo [f], Y. Favre [e], D. Ferrere [e], S. Gonzalez-Sevilla [e], K. Hanagaki [f], K. Hara [d], G. Iacobucci [e], Y. Ikegami [a], O. Jinnouchi [c], D. La Marra [e], K. Nakamura [a], R. Nishimura [b], E. Perrin [e], W. Seez [e], Y. Takubo [a], R. Takashima [b], S. Terada [a], K. Todome [c], Y. Unno [a], M. Weber [e]

[a] KEK, High Energy Accelerator Research Organization, Oho 1-1, Tsukuba, Ibaraki 305-0801, Japan
[b] Department of Science Education, Kyoto University of Education, Kyoto 612-8522, Japan
[c] Institute of Science and Engineering, Tokyo Institute of Technology, Ookayama 2-12-1, Meguro-ku, Tokyo 152-8551, Japan
[d] Institute of Pure and Applied Sciences, University of Tsukuba, Tsukuba, Ibaraki 305-9751, Japan
[e] DPNC, University of Geneva, CH 1211 Geneva 4, Switzerland
[f] Department of Physics, Osaka University, Machikaneyama-cho 1-1, Toyonaka-shi, Osaka 560-0043, Japan

ARTICLE INFO

Available online 15 May 2014

*Keywords:*
HL-LHC
ATLAS upgrade
Silicon
Strip module
Super-Module

ABSTRACT

Following successive upgrades of the CERN Large Hadron Collider (LHC) until approximately 2025, the High Luminosity LHC (HL-LHC) is expected to deliver pp collisions of centre-of-mass energy $\sqrt{s} = 14$ TeV with a levelled peak luminosity in excess of $5 \times 10^{34}$ cm$^{-2}$ s$^{-1}$ and an integrated luminosity of order 300 fb$^{-1}$ per year. The ATLAS Collaboration intends to replace the existing Inner Tracking Detector by a new tracker, with readout electronics as well as silicon pixel and strip sensor technology capable of maintaining the excellent mechanical and electrical performance of the existing tracker in the severe radiation and high collision rate environment of the HL-LHC. The super-module integration concept extends the proven design of the existing barrel silicon strip tracker to the HL-LHC, with double-sided stereo silicon micro-strip modules assembled into a low mass local support structure. The first phase of the Super-Module R&D programme has been successfully completed, demonstrating the feasibility of the Super-Module concept. A summary is made up of the key prototype mechanical and electrical results of the R&D, as well as a short perspective of future developments.


## 1. Introduction

Following successive upgrades until approximately 2025, the CERN Large Hadron Collider (HL-LHC) will deliver pp collisions at a centre-of-mass collision energy $\sqrt{s} = 14$ TeV, with levelled peak luminosities exceeding $5 \times 10^{34}$ cm$^{-2}$ s$^{-1}$ [1], with a 25 ns bunch spacing and with on average $\sim 140$ inelastic collisions per bunch crossing. In the following decade, the ATLAS experiment is expected to collect pp collision data corresponding to an integrated luminosity of order 3000 fb$^{-1}$.

The channel occupancy from the large track multiplicity expected per bunch crossing (more than 1000 tracks per rapidity unit), as well as the integrated radiation damage to the front-end electronics and sensors from the collision products, is beyond the performance capability of the existing silicon strip detector (SCT) [2]. The SCT was designed to operate at a peak luminosity of $10^{34}$ cm$^{-2}$ s$^{-1}$ up to an equivalent 1 MeV neutron fluence of $2 \times 10^{14}$ $n_{eq}$ cm$^{-2}$, compared with more than $5 \times 10^{14}$ $n_{eq}$ cm$^{-2}$ expected at the HL-LHC. For the HL-LHC, ATLAS intends to install a new Inner Tracking Detector (ITK) [3], with increased channel granularity and improved radiation hardness, to maintain or improve the track reconstruction efficiency and precision, as well as the b-tagging performance.

The Super-Module (SM) integration R&D project [4] discussed in this paper extends the proven merits of the existing barrel silicon strip tracker (SCT) [5] to the HL-LHC (mechanical and thermal stability, true stereo space-point reconstruction, sensor overlaps to provide offline alignment constraints using reconstructed tracks [6] amongst others). It also addresses some perceived design shortcomings. In the SM concept,[1] individual short-strip or long-strip double-sided stereo (DSM) modules are screwed to a light, stable carbon-fibre local support (LS) and inserted into the overall tracker support structure (Global Structure, GS). The LS holds at least 12

* Corresponding author.
*E-mail address:* Allan.Clark@cern.ch (A. Clark).

[1] The SM unit includes the LS fully loaded with DSM modules and their electrical and thermo-mechanical services.

http://dx.doi.org/10.1016/j.nima.2014.05.010
0168-9002/

DSM modules[2] depending on the layout, and allows full sensor hermiticity in $\phi$ and $z$.

The aims of the R&D project have been three-fold as follows:

(a) To minimise the material budget for the pixel and strip detectors. This objective applies not only to the DSM modules, but also to the services and power distribution, despite the vastly increased detector granularity.
(b) To demonstrate the reliable and reproducible electrical and mechanical fabrication and operation of so-called DSM250 modules using the prototype ABCN 250 nm CMOS front-end ASIC,[3] for the period of HL-LHC operation.
(c) To demonstrate a rigid but light CFRP[4] structure for the DSM modules, together with their thermo-mechanical and electrical services, that fulfils the HL-LHC requirements of stability and position accuracy.

To meet the aims of the project

(a) Prototype DSM250 modules have been constructed and successfully characterised thermo-mechanically, electrically, and with respect to irradiation [4,7], see Section 2. The construction procedure is also simplified with respect to the existing SCT modules, and is adapted for large-scale construction at multiple sites.
(b) Eight prototype DSM250 modules have been loaded onto an aluminium-based LS that accurately reproduces the positioning and electrical connectivity of the SM. The modules have been successfully read out simultaneously [8], see Section 3.
(c) A prototype demonstrator CFRP mechanical structure for the LS has been fabricated and successfully tested [9]. Either as specialised pieces or as part of the LS prototype, key attachment points have been tested, and the insertion of a SM has been fully validated. Using the proposed design for DSM130 modules, a detailed finite element (FEA)[5] model has been developed for thermal, thermo-mechanical and mechanical studies of the LS before and after loading with DSM modules and services [9], see Section 4.

Refs. [7–9] summarise the successful completion of the first phase of the SM R&D project. Section 5 briefly discusses further design and prototyping work (largely associated with the electrical services for DSM130 modules on a LS) that is still required to optimise a SM-based solution for the ATLAS barrel silicon strip tracker. Also in this section, the major steps foreseen for the next *preproduction* SM prototype using the DSM130 design are outlined.

Separate R&D projects address the development of radiation hard front-end readout integrated circuits (ICs) in 130 nm CMOS technology [10], and radiation tolerant silicon sensors [11] that are used by, but are largely decoupled from, the module design and the thermo-mechanical or readout techniques used in Refs. [7] through [9].

## 2. Double-sided silicon strip modules

The prototype DSM250 modules are described in Refs. [4,7]. Fig. 1 shows a prototype DSM250 short-strip (SS) module, and

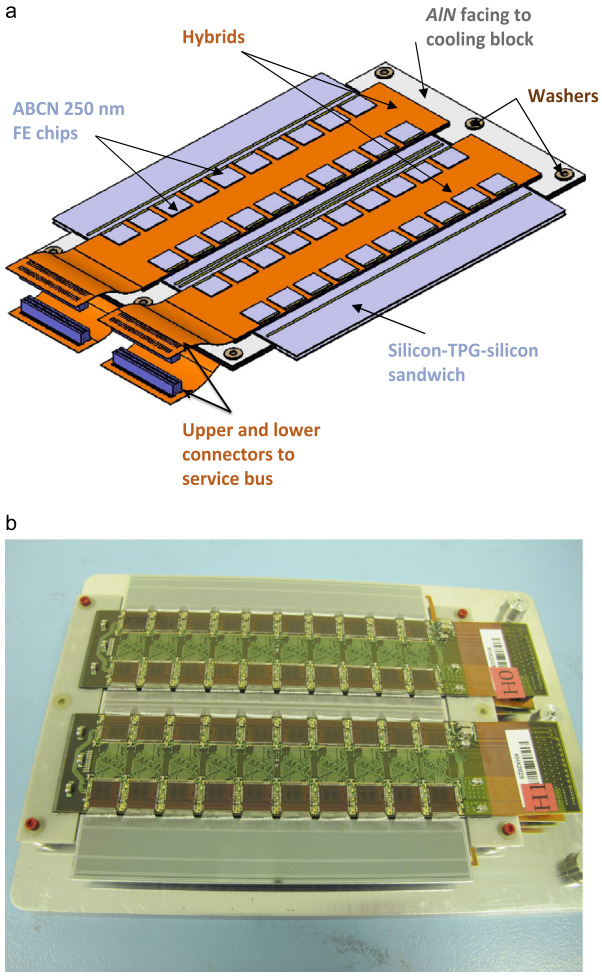


**Fig. 1.** (Upper) Schematic showing the major elements of the DSM250 module. (Lower) Upper-side photograph of a prototype DSM250 module. The active silicon sensor area is $96 \times 96$ mm$^2$.

Fig. 2 shows the 3D CAD design of the future DSM130 module. The design is a symmetric double-sided module with two $96 \times 96$ mm$^2$ n-on-p silicon micro-strip sensors glued to a central Thermal Pyrolitical Graphite (TPG) base-board. The DSM250 prototype has four bridged hybrids, each holding two columns of ten 128-channel readout ABCN 250 nm ICs [10], located as pairs on both sides of the module. Aluminium nitride (AlN) facings are located at each end of the base-board. The hybrid is a 4-layer copper-polymide (Cu/PI) flexible circuit designed at KEK. The sensors of the existing short-strip design are divided into four segments, two with axial and two with 40 mrad stereo strips of length $\sim 2.4$ cm and pitch 74.5 μm. The number of strips per segment is 1280, plus a guard strip at each end. The TPG base-board provides mechanical stability and ensures good thermal contact for heat dissipation to cooling blocks (Section 4). Long-strip modules are of identical design, but with less channels. The DSM130 module will be of similar design but with hybrids adapted for the 256-channel ABCN 130 nm CMOS IC.

The module extends and improves the existing SCT module design:

(a) The two sensors are mounted back-to-back allowing accurate space point reconstruction with a relative sensor alignment at the $\pm 1$ μm level. The modules are then centred and aligned precisely on the cooling plates of the LS using kinematic dowel fixations ($\pm 10$ μm).

[2] The current ITK baseline foresees 13 modules.
[3] Future DSM module prototypes (labelled DSM130 modules where relevant) will use the pre-production ABCN 130 nm ASIC that has recently been fabricated.
[4] CFRP: Carbon Fibre Reinforced Polymer layup providing a light structure with a controlled CTE, using successive layers (plies) of different carbon fibre orientation.
[5] ABAQUS Software from Simulia Dassault Systems, *Tool for multi physics FEA simulation*, see http://www.simulia.com/products/multiphysics.html.

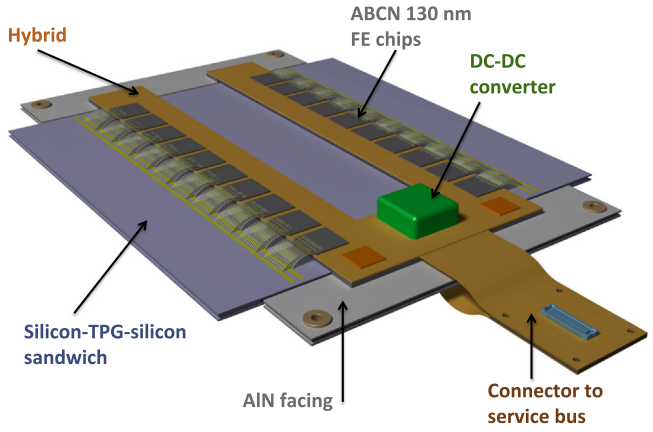


**Fig. 2.** The CAD design of the planned DSM130 module using the 256-channel ABCN 130 nm front-end ASIC, attached to the cooling plates and the LS. The active silicon sensor area is $96 \times 96$ mm$^2$.

(b) The hybrid and sensor thermal paths are independent. The use of materials with low thermal expansion (CTE) and good thermal conductivity minimises deformations during temperature cycling. Detailed finite element (FEA) calculations exist (Section 4) indicating a maximum longitudinal deviation of less than 15 μm for a temperature change between room temperature and −35 °C. The sensor temperature is sensitive to the contact with the cooling plates of the SM design. For the pessimistic case of thermal contact at the attachment screws, the existing module prototype can be maintained with a temperature difference of 11–13 °C with respect to $CO_2$ cooling tubes at −35 °C. FEA calculations indicate an additional temperature increase of ∼4 °C if the hybrid is directly glued to the sensors. For DSM130 modules with a thermal grease contact along the length of the cooling plate, and ambient convection cooling at 0 °C, the temperature difference is reduced by several degrees (Section 4).

Sixteen DSM250 modules have been constructed at KEK (Japan) and the University of Geneva (UniGe), including one half-module used for radiation studies. Production has been industrialised at KEK. The noise level for directly powered modules in a DSM test box is typically between 575 and 600 electrons equivalent noise charge (ENC) at 1 fC input charge, measured at 250 V bias and a module temperature of approximately 35 °C [7], see Fig. 3. The noise uniformity is at the level $\sigma \sim 25$ ENC. The performance of the modules has been tested to be stable for bias voltages of beyond 500 V, over a range of temperatures.

Proton irradiation tests were also made at −10 °C on a single-sensor module at the CERN PS irradiation facility [12]. The 1 MeV neutron equivalent fluence recorded varied between $3 \times 10^{14}$ $n_{eq}$ cm$^{-2}$ and $1.4 \times 10^{15}$ $n_{eq}$ cm$^{-2}$. Despite a leakage current increase of 5–6 orders of magnitude, the noise increase was small. Data from single-sided modules of an alternative ATLAS base-line construction concept [13] confirmed this result. However, no data from test beams or from radioactive sources are available.

## 3. Electrical performance of a super module prototype using DSM250 modules

The benchmark SM concept for the barrel strip detector foresees DSM modules attached to a light, stable carbon fibre local support that is end-inserted into an overall support structure. Depending on the final ITK layout, the local support will hold 12 or 13 modules. It is essential to verify this concept mechanically, thermo-mechanically and electrically.

DSM250 modules have been used for a prototype electrical SM, constructed from aluminium, and loaded with 8 modules, as well as first-generation cable buses and prototype hybrid controller boards. The connectivity and geometrical arrangement is close to that foreseen for a production SM unit. In this prototype, shown in Fig. 4, the high-voltage distribution is individual, but the digital voltage for the ABCN 250 nm IC readout is provided using prototype DC–DC converters [14]. The analog voltage of the ABCN 250 nm IC front-end is provided from the digital voltage using on-chip linear voltage regulators. A total of 81 920 channels are read by the data acquisition, by far the largest multi-module system so far using the ABCN 250 nm IC.

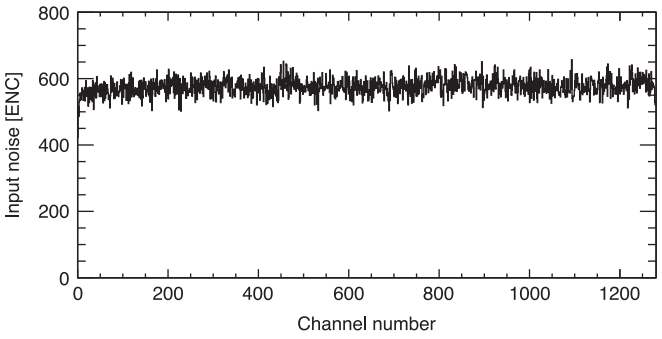


**Fig. 3.** Measured ENC noise for each channel of a typical hybrid for DSM250 modules.

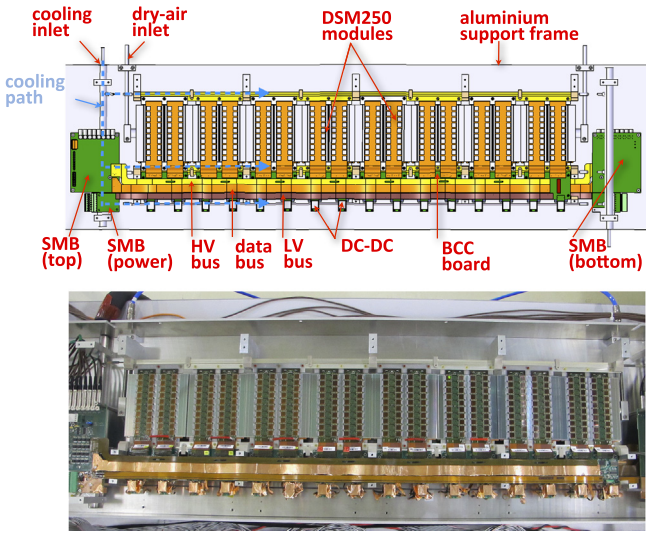


**Fig. 4.** Schematic (upper) and photograph (lower) of electrical SM prototype with the 8 DSM250 modules read via a cable bus to a SM Controller card. The DC–DC converters are also visible. Taking account of a 1 mm active overlap between modules, the total active length of the SM electrical prototype is 761 mm.

The electrical SM prototype characterisations have been successfully completed and detailed in Ref. [8]. Selected results are noted below:

(a) The sensor bias voltage in this case has been supplied individually to each side of each module. In three modules, pin-holes in the TPG coating resulted in coupling between the 2 sides. Future designs will use a single bias channel for several modules, to reduce the service material. The modules used a common low-voltage line, and either DC–DC conversion or serial powering is foreseen for the final DSM modules. In the case of DC–DC converters,[6] despite a 10 μm Cu shielding,

[6] The DC–DC converter development is ongoing and the converters used were early prototypes.

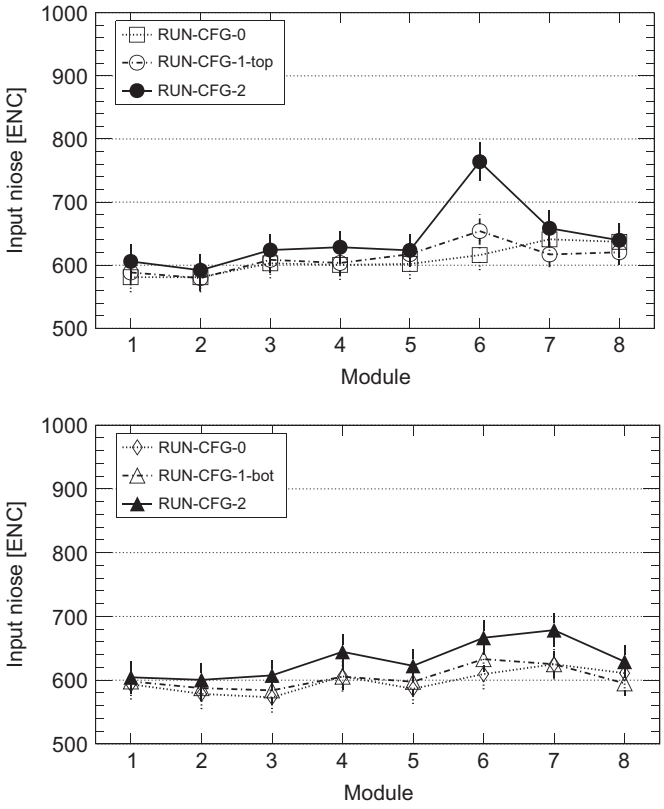


**Fig. 5.** The mean ENC, together with the channel-by-channel Gaussian spread of ENC, measured for each side of each module for the cases of single module readout (CFG-0); top-side or bottom-side read-out for all 8 modules with the DC–DC converters on the other side disabled (CFG-1 top or bottom); and all channels measured simultaneously with all DC–DC converters enabled (CFG-2).

electromagnetic emissions (primary frequency 2 MHz) were observed. In future prototypes, the shielding will be an important issue.

(b) Following channel-by-channel gain and threshold calibrations, the output noise of each channel has been measured. Data were collected at a sensor (hybrid) temperature of approximately 20 (32) °C. Three sets of measurements have been made: each side of each module measured individually (CFG-0); the top-side or bottom-side channels of the 8 modules read out, with the DC–DC converters on the other side disabled (CFG-1 top or bottom); and finally the case of all channels measured simultaneously (CFG-2). The resulting mean and spread of ENC for each side of each module are shown in Fig. 5. With the exception of module 6, the increased ENC for full simultaneous readout was in the range 10–60 ENC. The deteriorated performance of 2 hybrids in module 6, and a deteriorated common mode noise for module 7 as evidenced by the noise occupancy, is not fully understood, but is related to pickup from the DC–DC converter emissions. While these results are extremely promising, further shielding optimisation is needed for the future SM prototype using DSM130 modules.

(c) Noise occupancy (NO) measurements of the probability for a given strip to record a signal due to noise have been made. For a 100 mV threshold,[7] the NO level is at most $10^{-8}$, excepting one side of module 7 in the CFG-2 configuration that showed a significant increase in common-mode noise, due presumably to the coupled effect of the top- and bottom-side DC–DC converters.

(d) Double Trigger Noise (DTN) [15] measurements to measure the effect of injecting 2 closely spaced triggers with read out thresholds of successively 0.5 fC, 0.75 fC and 0.5 fC. For a spacing close to the IC pipeline length, the second trigger will record the occupancy of the module as the readout of the first trigger starts. As no charge is injected, no hits should be recorded. This is almost always the case. However, for a 0.5 fC threshold in the CFG-2 configuration, there is a large increase in the number of recorded hits, again indicating common-mode noise resulting from the coupling of the top- and bottom-side DC–DC converters.

In summary, the electrical performance of the 8-DSM electrical SM has been fully characterised, and the multi-module readout has been successfully demonstrated. Results have been presented [8] of the ENC noise, NO and DTN. The data are extremely satisfactory and largely according to the design expectation of the ABCN 250 nm IC. However, in some modules when all of the 32 DC–DC converters are enabled, an increase of common-mode noise is measured. In future SM developments using DSM130 modules (Section 5), particular attention must be paid to improve the shielding of the DC–DC converters.

## 4. Super module mechanics

The current SM design foresees that a row of DSM modules, together with their thermal and electrical services, will be mounted on a light, stable CFRP support (LS) that can be inserted longitudinally and without stress on a support cylinder. The emphasis of the design has been to minimise thermo-mechanical stresses while maintaining excellent build and placement precision and a minimal material budget. As summarised in Ref. [9], R&D has concentrated on the development of a prototype LS satisfying the ITK requirements [3] and the development of a detailed FEA model to allow an optimisation of the LS and SM design. The design aims to maintain or exceed the stability specifications of the existing SCT [2], while significantly reducing the material budget.

Fig. 6 shows a 3D CAD perspective and a cross-sectional view of the FEA model describing the LS and fully loaded SM (in this case using DSM130 modules).

The exploded view of Fig. 7 (upper) shows the individual components of the LS. The components are glued together in precision jigs with an expected room-temperature precision of order $\pm 10$ μm. A schematic of the assembled LS attached to the global structure (GS) cylinder is shown in Fig. 7 (lower). The prototype LS has been fabricated using T300 fibre CFRP layups.[8] Photographs of the assembled LS prototype are shown in Fig. 8.

The precision assembly of DSM250 modules on aluminium cooling plates has been fully tested [8,9]. The cooling plates are then precision mounted on the LS backbone. In the baseline design, the plates are made from Carbon–Carbon (C–C) with 2-dimensional plies, CC2D,[9] that are screwed onto the PEEK pads of the LS wings (the precision of this step requires validation). Other tailor-made CFRP layups are also being considered. To minimise the stress from different plate and pipe CTE, the pipe is able to move freely

[7] A 1 fC input charge corresponds to a calibrated signal in the range 130–150 mV.

[8] T300 fibres have been used for prototype studies but M55J fibres are being considered for future pre-production prototypes. Toray Corporation, Japan.

[9] CC2D is a carbon-fibre-epoxy 2-directional (0–90°) fabric that is fired at high temperature to form a C–C ceramic, with the mechanical strength of carbon-fibre and thermal conductivity of carbon in the plane of the fabric. JX Nippon Oil and Energy Corporation, Japan.

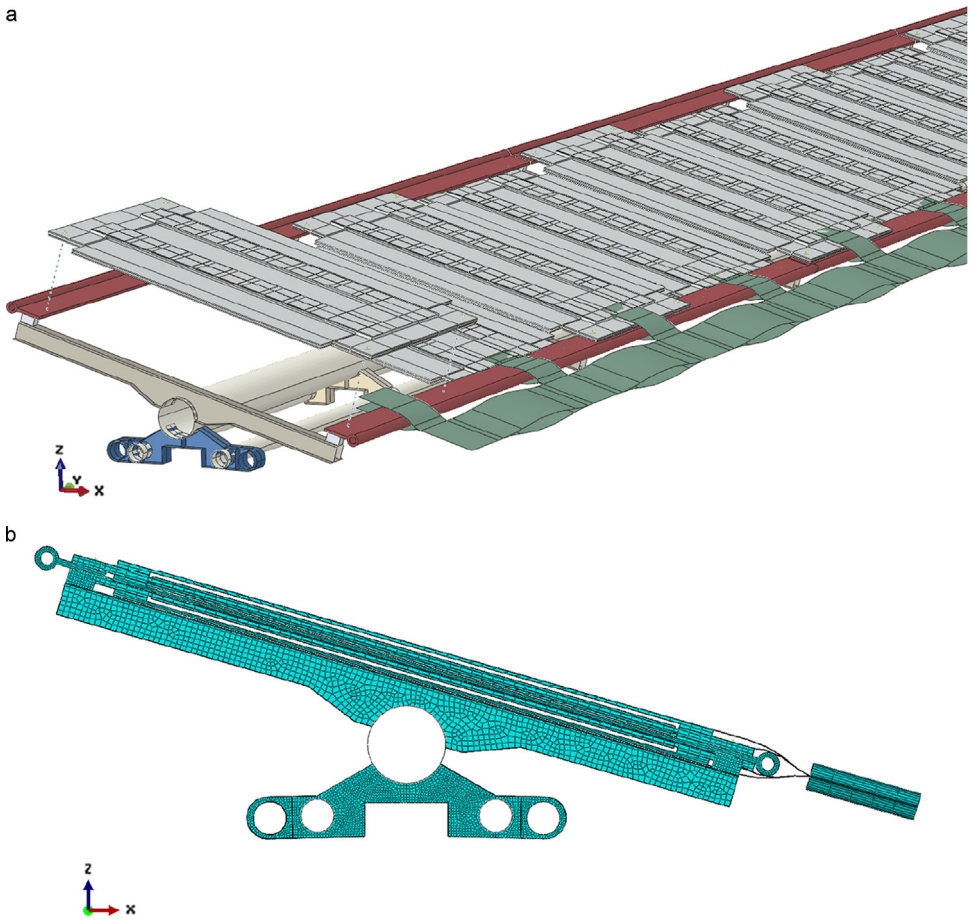


**Fig. 6.** (Upper) A 3-dimensional perspective of the SM used as input for FEA analyses. The central tube and wings of the LS are shown in grey, and the cooling plates are shown in red. The DSM130 modules are shown in grey; one DSM130 module has been removed from the LS to show details of the structure. The electrical service bus is shown in blue. (Lower) A cross-sectional view of the fully loaded SM. (For interpretation of the references to colour in this figure caption, the reader is referred to the web version of this paper.)

with a high thermal conductivity, radiation hard grease thermal contact.[10] Conductive grease is also used to ensure thermal contact between the module facing and the cooling plate.

The electrical service bus is also attached to the LS wings (see Fig. 6). A prototype service bus has already operated in the prototype electrical SM [8]. An optimised design for DSM130 modules is under development, see Section 5. A key issue is to limit thermal stresses from the service bus onto the modules; this is discussed in FEA studies below.

The LS design currently foresees 3 kinematic fixation points along the $\sim$1275 mm SM length. These are located in Fig. 7 at $z=0$ mm (allowing for longitudinally sliding), at $z\sim 600$ mm (also longitudinally free) and at $z\sim 1200$ mm where all degrees of freedom are constrained to limit mechanical stresses from service connections. The longitudinal sliding of the other fixation points prevents stresses from GS movements or small CTE mismatches between the LS and GS (both structures have minimal CTE). The fully loaded prototype LS of Fig. 8 (lower) has been attached to a mock-up of the GS using fixation points fabricated from PEEK. This has allowed a full validation of the end-insertion feature of the LS design.

A detailed FEA model of a fully loaded SM, using DSM130 modules and an optimised LS design, has been used to quantify the expected mechanical and thermo-mechanical deformations. This FEA model has been used to generate the SM perspective of Fig. 6. The DSM130 modules have a detailed model definition: silicon wafers on each side of a TPG element with appropriate glue layers, a detailed hybrid definition based on the ABCN 130 nm IC, and an AlN base plate with a thermal grease contact to the cooling plate. The same thermal grease is applied between the cooling pipes and the cooling plates. The thermal grease is modelled using a conservative Young Modulus of 230 MPa, an over-estimate of stresses in the LS following an integrated radiation dose expected for the HL-LHC ATLAS silicon strip tracker. A conservative solution, assuming no thermal grease between the DSM module and the cooling plate, is also studied. The kinematic links between the modules and cooling plate, and between the LS and the global structure, are included. The service bus assumes the material properties as used for the IBL service bus. Details of the assumed material and thermal properties, and the different material options considered, are described in Ref. [9].

The FEA models assumes an initial steady-state temperature of $T=20$ °C for all components. The final steady-state temperatures assume a coolant temperature of $T=-35$ °C, powered sensor and on-detector electronics, and dry air circulation at $T=0$ °C. Details of the assumed material and thermal properties, and the different material options considered, are described in Ref. [9].

A simplified model using material properties of the loaded prototype SM has been compared with deflection measurements

[10] The most promising grease candidate is the non-silicone, ZnO-filled HTCP grease, see www.electrobe.com. Adequate thermal and mechanical behaviour is maintained beyond the irradiation requirements of the ITK, nevertheless other greases are being evaluated.

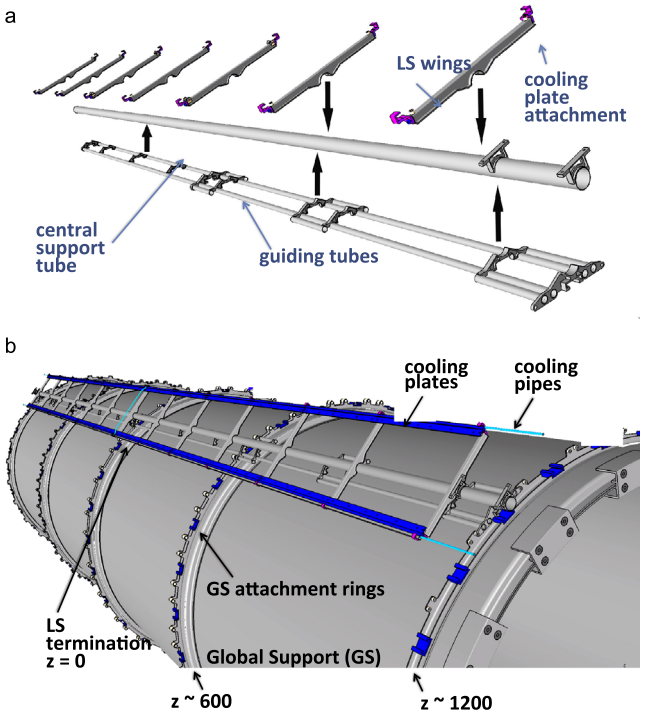


**Fig. 7.** (Upper) Exploded view of the LS CFRP components, including the 7 module and service attachment wings, the central support tube, and the LS attachments to the global structure. (Lower) View of 2 assembled LS units on a barrel with attachment points at 3 points along the LS length (nominally at $z=0$ mm, $z\sim 600$ mm and $z\sim 1200$ mm). The attachment at $z=0$ mm is designed to capture the LS units inserted from each end of the GS. The CC2D cooling plates and titanium alloy cooling tubes are added for clarity, but the DSM modules and the service bus are not shown.

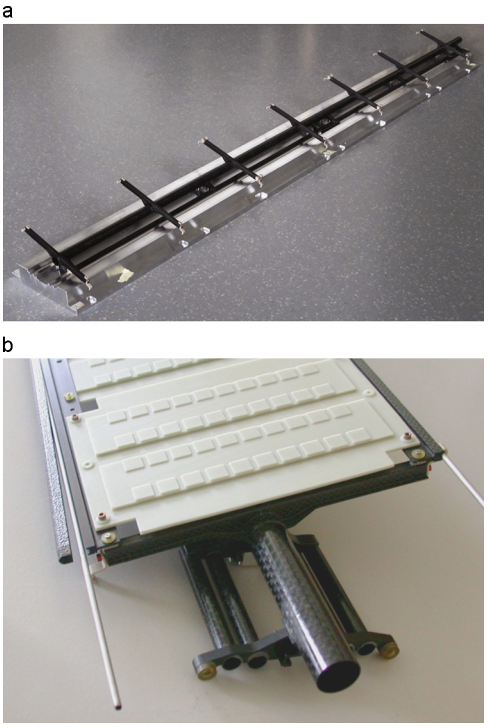


**Fig. 8.** Photograph of the assembled prototype LS on its jig, before being equipped with the cooling plates, service bus and DSM modules (upper). Photograph after assembly of the cooling plates, cooling tubes and dummy DSM250 modules (lower).

using a 1 kg force perpendicular to the sensor surface. The expected FEA deflection of 0.5–0.6 mm can be compared with a maximum measured deflection of 0.65 mm.

Several options are quoted in Ref. [9]: the results quoted in this report concern base-line steady state operational conditions with a gravitational loading perpendicular to the plane of sensor surface (configuration 2 in Ref. [9]). Taking into account the effect of the service bus, but ignoring its own larger deformation, the maximum out-of-plane deflection due to the combined mechanical and thermo-mechanical stresses is $\sim 55$ μm (largely gravitational), with maximum in-plane distortions (largely thermo-mechanical) of 15 μm. The deflection is sensitive to the number of attachment links, and to the details of the CFRP backbone tube (a 5-ply CFRP layup of M55J fibre is assumed). For a 3-ply layup, the out-of-plane deformation increases to $\sim 70$ μm. Detailed optimisations of the material budget with respect to the maximum deformation are in progress. A mapping of the deflection is shown in Fig. 9. As expected, the maximum deflection is midway between the global support links.

While the temperature uniformity of the sensors during operation is small ($\Delta T$ less than $\sim 0.5$ °C for a loaded SM as shown in Fig. 10), the operational temperature is sensitive to the thermal barriers between the sensor and the coolant. For a perfect 50 μm grease contact between the module and cooling plate, the mean sensor temperature is expected to be $T=-31$ °C. In the case of a direct contact between the module and the cooling plate only at the attachment screws, the mean sensor temperature is increased by $\Delta T\sim 5$ °C. If the module hybrid is glued directly to the sensor, the mean sensor temperature is also expected to increase by $\Delta T\sim 4$ °C. Even if both extremes are applied, stable operation is assured for the full operational period with a sensor temperature of less than $T=-20$ °C.

## 5. Future super module R&D perspective

Both mechanically and electrically, the first phase of the SM R&D project has been completed. Future developments will use the 256-channel ABCN 130 nm CMOS ASIC that has recently been fabricated, as well as a new Hybrid Control Chip (HCC) in 130 nm CMOS technology that is now under design and will be submitted for fabrication in 2014.

The next phase of this project should aim to demonstrate a multi-module pre-production SM:

(a) Using the most recent prototype n-in-p sensors and the 256-channel ABCN 130 nm IC, several DSM130 modules following the design of Fig. 2 will be fabricated. The DSM130 prototypes will initially be compatible with DC–DC powering (serial powering remains an alternative) and with a multi-module sensor bias line. The DSM130 hybrid is now under design at KEK. Special attention will be given to final material optimisation, and to the DC–DC converters. Averaged over the SM active area, the total module material is expected to be 1.59% $X_0$. The modules will be individually characterised in a modified version of the existing single-module test box.

(b) Subject to satisfactory performance, at least 8 DSM130 modules will be fabricated in industry. The existing electrical SM structure will be modified to support the DSM130 prototypes. The major change will concern the design and fabrication of a new very compact and low mass service bus, and the implementation of the HCC hybrid controller, as well as a prototype end-of-SM controller board (SMC), not necessarily of the final geometric layout. The service bus design will be based on that of the IBL stave flex [16]. The current design assumes a 20 mm width, except in the module connector region (22 mm) to allow for low-voltage bias and interconnections between the Al and Cu substrates. The two 50 μm thick Al layers will be tapered between 11 mm and 20 mm in width. The Cu layers

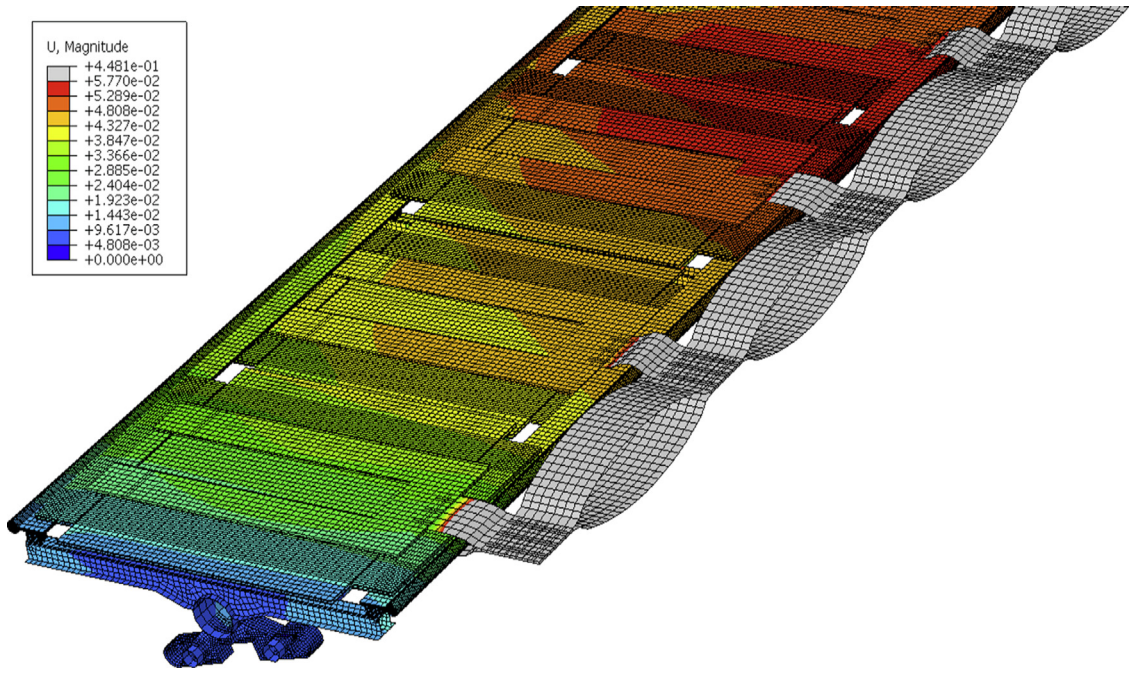


**Fig. 9.** Mapping of the total deformation due to the combined effects of gravitational load and thermal operational conditions for 4 modules of the SM. As expected, the maximum deflection is midway between the global support attachments. The displacement scale is in the range 0 μm (minimum, blue) to 57.7 μm (maximum, red), not considering the larger cable-bus displacement. (For interpretation of the references to colour in this figure caption, the reader is referred to the web version of this paper.)

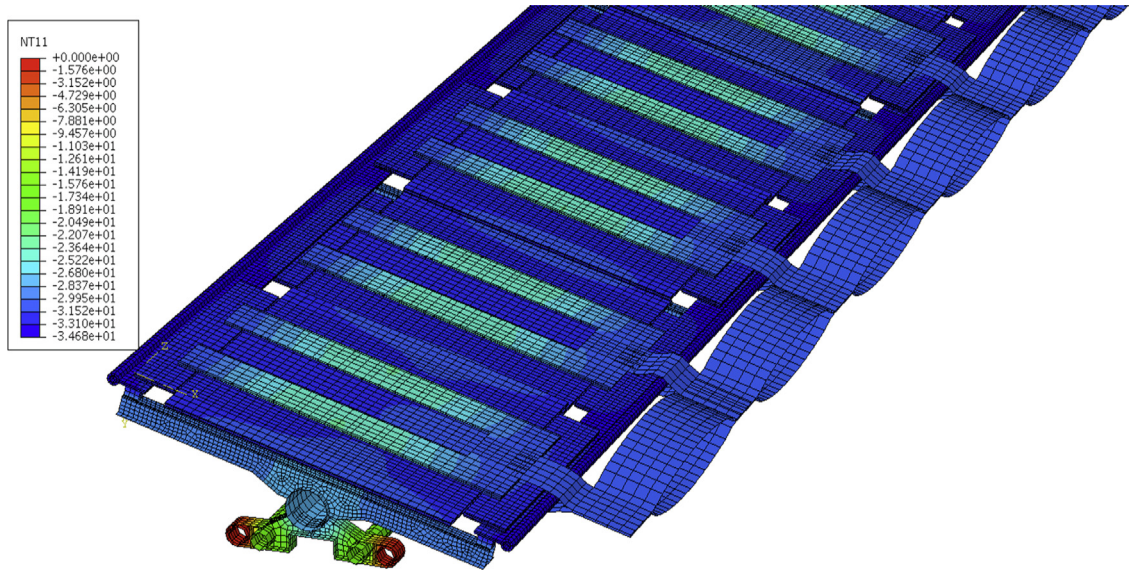


**Fig. 10.** Mapping of the temperature on the SM, assuming steady-state operation with a $CO_2$ coolant temperature of $-35$ °C. The temperature scale is in the range $T=-35$ °C (blue) and $T=0$ °C (red). (For interpretation of the references to colour in this figure caption, the reader is referred to the web version of this paper.)

will consist of two 15 μm thick layers to carry the LVDS, HV and DCS signals and one 5 μm thick Cu mesh to control the LVDS impedance.

(c) On the basis of the service bus performance, the bus design will be extended to be attached on a CFRP LS (averaged over the SM active area, the total service material is expected to be 0.11% $X_0$). As discussed in Section 4, an FEA model will be used for a material and design optimisation of the LS components, prior to the fabrication of a second-generation LS (expected material budget 0.18% $X_0$ and 0.26% $X_0$ including the cylinder interface brackets and inserts). Averaged over the active DSM area, the total material is 2.17% $X_0$ (1.91% $X_0$) including (excluding) the LS and cylinder interface. The nominal specification for the maximum material budget is 2% $X_0$, excluding the support structure but including the service bus.

(d) Ideally, as a final step, a multi-module electrical test, as well as test beam studies, will be made for a fully assembled SM using this LS.

The most challenging issue is the electrical and mechanical optimisation of the service bus. Fortunately, an advantage of the SM design is that this optimisation can be factorised from other pre-production prototyping.

## 6. Conclusions

A Super Module integration R&D program for the upgraded ATLAS Inner Tracker at the proposed HL-LHC [4] has completed the first phase of a feasibility study. The results detailed in Refs. [7–9] and summarised in this presentation demonstrate the feasibility of the Super Module concept. Work towards a realistic preproduction prototype is well advanced, taking into account prototype evolutions of the sensor and front-end IC design. A key issue is the optimisation and characterisation of the service bus and power distribution for the super-module, aiming to minimise the material budget while maintaining the mechanical and electrical integrity and the long-term operational robustness.

## Acknowledgments

The authors acknowledge the support of the funding authorities of the collaborating institutes, including the JSPS Grant-in-Aid for Scientific Research (A) [Grant 20244038], the MEXT Grant-in-Aid for Scientific Research in Priority Area [No. 20025007] and on Innovative Areas [No. 23104002], Japan, as well as grants from the Swiss State Secretariat for Education, Research and Innovation, the Swiss National Science Foundation and the Canton of Geneva.

## References

[1] L. Rossi, LHC Upgrade Plans: Options and Strategy, CERN-ATS-2011-257.
[2] G. Aad, et al., ATLAS Collaboration, Journal of Instrumentation 3 (2008) S08003.
[3] The ATLAS Collaboration, Letter of Intent for the Phase-II Upgrade of the ATLAS Experiment, CERN-LHCC-2012-022, 2012.
[4] S. Gonzalez-Sevilla, et al., A silicon strip module for the ATLAS Inner Detector upgrade in the Super LHC Collider, in: Proceedings of the 7th International "Hiroshima" Symposium on the Development and Application of Semiconductor Tracking Detectors (HSTD7), Hiroshima, Japan, Nuclear Instruments and Methods in Physics Research Section A 636 (2011) S97.
[5] S. McMahon, on behalf of the ATLAS Collaboration, Operation and Performance of the ATLAS Semiconductor Tracker, JINST 9 (2014) P08009.
[6] ATLAS Collaboration, Alignment of the ATLAS inner detector tracking system with 2010 LHC proton–proton collisions at $\sqrt{s}=7$ TeV, in: ATLAS Conference Note ATLAS-CONF-2011-012; ATLAS Collaboration, Study of alignment-related systematic effects on the ATLAS inner detector tracking, in: ATLAS Conference Note ATLAS-CONF-2012-141.
[7] G. Barbier, et al., Design and assembly of double-sided silicon strip module prototypes for the ATLAS upgrade strip tracker, ATLAS Public Note ATL-UPGRADE-PUB-2011-002, 2011; S. Gonzalez-Sevilla, et al., Electrical results of double sided silicon strip modules for the ATLAS upgrade strip tracker, ATLAS Note ATL-UPGRADE-PUB-2012-002, 2012.
[8] S. Gonzalez-Sevilla, et al., Journal of Instrumentation 9 (2014) P02003.
[9] G. Barbier, et al., Mechanical studies towards a silicon micro-strip super module for the ATLAS inner detector upgrade at the high luminosity LHC, Journal of Instrumentation 9 (2014) P04018.
[10] F. Anghinolfi, et al., Performance of the ABCN-25 readout chip for the ATLAS inner detector upgrade, in: Proceedings of Topical Workshop on Electronics for Particle Physics (TWEPP-09), Paris, France, CERN-2009-006, p. 62.
[11] Y. Unno, et al., Development of n-on-p silicon sensors for very high radiation environment, in: Proceedings of the 7th International "Hiroshima" Symposium on the Development and Application of Semiconductor Tracking Detectors (HSTD7), Hiroshima, Japan, Nuclear Instruments and Methods in Physics Research Section A 636 (2011) S24.
[12] M. Glaser, et al., Nuclear Instruments and Methods in Physics Research Section A 426 (1999) 72.
[13] S. Diez, Silicon strip staves and petals for the ATLAS Upgrade tracker of the HL-LHC, in: Proceedings of the 8th International Symposium on the Development and Application of Semiconductor Tracking Detectors (HSTD8), Taipei, Taiwan, Nuclear Instruments and Methods in Physics Research Section A 639 (2013) S93.
[14] A. Affolder, et al., Journal of Instrumentation 6 (2011) C11035.
[15] P.W. Phillips, Nuclear Instruments and Methods in Physics Research Section A 570 (2007) 230.
[16] ATLAS Collaboration, ATLAS Insertable B-Layer Technical Design Report, Technical Report, CERN-LHCC-2010-013, ATLAS-TDR-019, CERN, Geneva, September 2010.